IOPscience iopscience.iop.org

Home Search Collections Journals About Contact us My IOPscience

Modelling the structure of GaAs and InAs nanowires

This article has been downloaded from IOPscience. Please scroll down to see the full text article.

2008 J. Phys.: Condens. Matter 20 454226

(http://iopscience.iop.org/0953-8984/20/45/454226)

View the table of contents for this issue, or go to the journal homepage for more

Download details:
IP Address: 129.252.86.83
The article was downloaded on 29/05/2010 at 16:13

Please note that terms and conditions apply.

IOP PUBLISHING JOURNAL OF PHYSICS: CONDENSED MATTER
J. Phys.: Condens. Matter **20** (2008) 454226 (6pp) doi:10.1088/0953-8984/20/45/454226

Modelling the structure of GaAs and InAs nanowires

M Galicka, M Bukała, R Buczko and P Kacman

Institute of Physics, Polish Academy of Sciences, Aleja Lotników 32/46,
02-668 Warsaw, Poland

E-mail: galicka(at)ifpan.edu.pl

Received 13 May 2008, in final form 16 July 2008
Published 23 October 2008
Online at stacks.iop.org/JPhysCM/20/454226

Abstract
Using *ab initio* methods, we study the stability of thin (diameters up to 10 nm) GaAs and InAs nanowires. Modelled nanowires were constructed using bulk atomic positions along six different crystallographic directions of either zinc-blende or wurtzite structures. Taking into account the reconstruction of the nanowire surfaces, we have found that, for diameters of up to 50 Å, the most stable nanowires adopt the wurtzite (0001) structure—for such diameters the free energy of zinc-blende nanowires along any crystallographic axis is always larger than that of the wurtzite (0001) ones. To calculate the free energy in nanowires with larger diameters, we have approximated their total energy by the sum of congruous bulk and bulk surface energies. In these nanowires the interplay between the wurtzite and zinc-blende structures was demonstrated. The band structure and the density of charge in the nanowires have also been calculated.

(Some figures in this article are in colour only in the electronic version)

1. Introduction

The tremendous and constantly growing interest in nanowires (NWs), i.e. needlelike nanocrystals, is stimulated by the recent discoveries that such one-dimensional structures can be used as building blocks of various nanoscale electronic and photonic devices. Nanoscale field-effect transistors [1–5], inverters [4, 5] and logic gates [5] are some examples of NW-based devices. One-dimensional electronics can also take advantage of the growth of heterostructures along the NW axis, as has been demonstrated in resonant tunnelling diodes [6] and single-electron transistors [7].

A theoretical description of the properties of NWs is essential for an understanding of the fundamental physics underlying their behaviour and hence for further development of one-dimensional nanotechnologies. Importantly, adequate growth models which recognize the thermodynamic driving forces for III–V NW formation during catalyst-assisted growth by MBE and other methods have been already proposed [8, 9]. On the other hand, it seems that the free energy is the most important parameter which determines the stability of the final structure. Several more or less simplified models have been proposed for free energy calculations and studies of the mutual stability of NWs of zinc-blende zb(111) and wurtzite wz(0001) structures. In [10] the energies for NWs of six different chemical compositions have been obtained and compared within an empirical interatomic potential model. In this approach, however, the possible bonding reconstruction at the lateral surfaces and dangling bonds saturation by foreign atoms was not taken into account. The wz and zb NWs with saturated and clean facets have also been compared by *ab initio* (density functional theory (DFT)) methods, but again without the bonding reconstruction [11]. The structural stability of NW with full bonding reconstruction, still without dangling bond passivation, has been studied by Akayama *et al* [12] by DFT methods, but only in the case of InP NWs. Finally, it should be mentioned that in [8] a simple counting of the number of dangling bonds on lateral facets and an estimation of their energy input allowed the authors to predict various possible stacking sequences and polytypes of wz(0001) and zb(111) structures.

In general, the results of the above-mentioned models show the crucial role of the lateral surface energy for the stability of the structure. In all the studied NWs, the number of dangling bonds at the clean nonsaturated surfaces is larger for zb than for wz—this leads to higher lateral surface energy for zb and, thus, to lower free energy for wz structures. The contribution of the lateral surface to the total free energy

 © 2008 IOP Publishing Ltd Printed in the UK

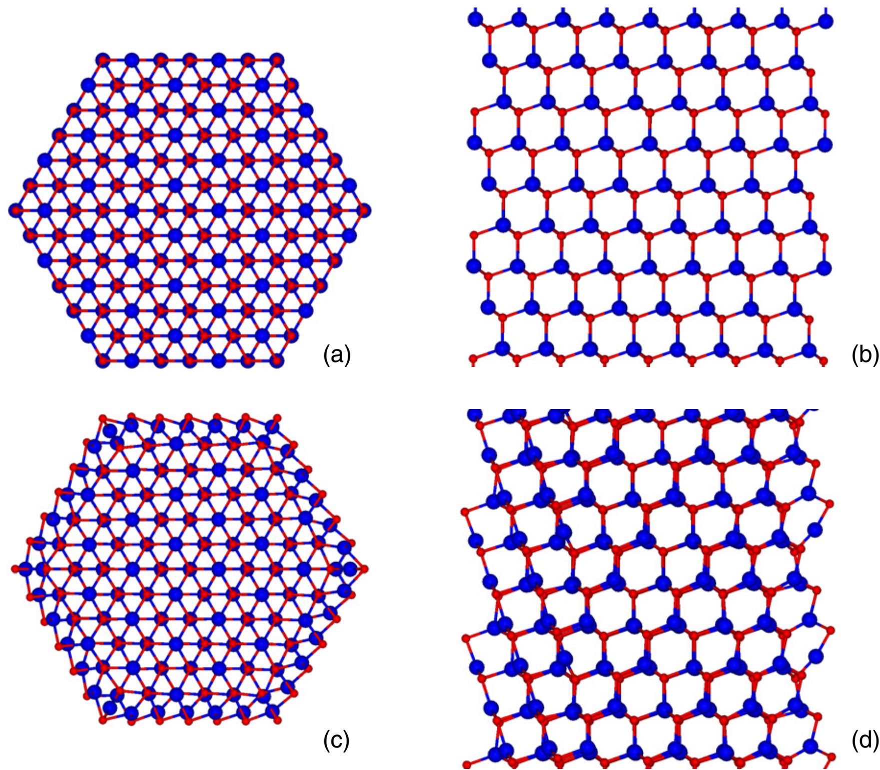

Figure 1. An InAs zb NW grown along the (111) direction. The diameter of the NW is about 30 Å. The blue (black) and red (gray) circles denote In and As atoms, respectively. The NW before the relaxation—(a) top and (b) side view. The NW after the relaxation—the view from the top (c) and from the side (d).

diminishes. However, with increasing NW diameter, and for some critical diameter, the inside volume cohesive energy (which in the case of GaAs and InP is, in contrast, lower for zb than for wz) becomes more important. The critical diameter is compound-dependent and numerical estimates give the values 112 Å for GaAs [10] and 120 Å for InP [12].

In this paper we present the results of a careful theoretical investigation of the stability and band structure of GaAs and InAs nanowires, in which full bonding reconstruction is allowed. We consider infinite NWs of both zinc-blende (zb) and wurtzite (wz) structure, grown in various crystallographic directions. Our calculations are performed for zero pressure and zero temperature with the use of the *ab initio* DFT method and we assume that the surface atoms on the facets are not saturated by foreign, e.g. hydrogen, atoms.

2. Model nanowires—surface reconstruction

At first, we study NWs with diameters ranging from 6–50 Å oriented along different crystallographic axes. Our model NWs are cut out from the bulk—in the zb structure along the three, (001), (110) and (111) crystallographic directions; in the wz structure along the (0001), $(10\bar{1}0)$ and $(\bar{1}100)$ axes. The periodic boundary conditions are employed along the NW growth axis. Due to the calculation method described below, we use also periodic conditions in the other two directions, with the unit cell dimensions ensuring that minimum separation between neighbouring wires is not less than 10 Å. This creates, in effect, a net of separated continuous wires. Examples of the wires constructed in the above described way are shown in (a) and (b) of the first two figures—an example of zb NW is presented in figure 1 and of wz NW in figure 2.

Then, we use first-principles methods to determine the atomic configuration corresponding to the minimum energy of each of the initial structures. We allow for relaxation of all atomic positions and of the unit cell dimension along the NW axis. The resulting structures are shown in parts (c) and (d) of the same figures. The main visible effect of the relaxation procedure is the interatomic bonding reconstruction at the NW side surface. As one can see in the figures, the shape of the NW surface changes considerably after the relaxation. This is mainly due to the change of positions of cations, i.e. Ga or In atoms, which during the surface reconstruction are tending to a planar configuration.

In the *ab initio* calculations reported here the VASP code [13, 14], which is based on the density functional theory (DFT), has been used. After performing various tests of the convergence, i.e. with respect to cutoff energy, k points and distances between the NWs in neighbouring cells (vacuum regions), in our calculation we adopt a plane wave basis set with a 13 Ryd cutoff energy. For the atomic cores the norm-conserving nonlocal, ultrasoft pseudopotentials of Perdew–Wang 91 [15] are used. The k points are generated with a $(1 \times 1 \times n)$ mesh, where $n \geqslant 50$ Å$/c$ and c is the unit cell dimension in the growth direction. The exchange correlation energy is calculated using the generalized gradient

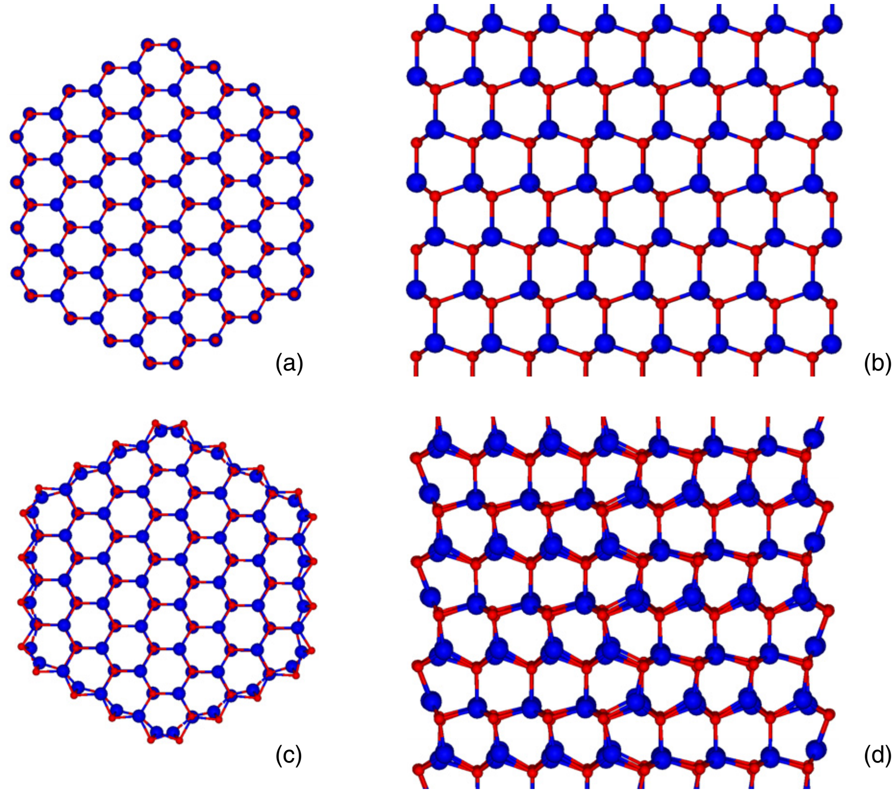

Figure 2. An InAs wz NWs along the (0001) direction, with the diameter equal to about 30 Å. The blue (black) and red (gray) circles denote In and As atoms, respectively. The NW before the relaxation—top (a) and side (b) view. The NW after the relaxation—the view from the top (c) and from the side (d).

approximation and the atomic coordinates are relaxed with a conjugate gradient technique. To determine the equilibrium configurations the criterion that the maximum force is smaller than 0.01 eV $Å^{-1}$ is used (this corresponds to a change in the total energy per pair smaller than 2×10^{-6} eV).

In order to find the most energetically favourable nanowire structures we compare their wire free energies. The free energy per cation–anion pair is defined as

$$\varepsilon_{\text{free}} = \varepsilon_{\text{wire}} - \mu_{\text{bulk}}^{\text{zb}}, \quad (1)$$

where $\varepsilon_{\text{wire}}$ denotes the NWs total energy (E_{wire}) divided by the number of atomic pairs in the wire. To compare the free energies of wurtzite and zinc-blende wires with the same value, we use in both cases $\mu_{\text{bulk}}^{\text{zb}}$—the energy per anion–cation pair in the bulk of the zb structure, i.e. in the crystallographic structure typical for InAs and GaAs bulk materials. We note that $\varepsilon_{\text{free}}$ is always positive, because it reflects the energy cost of the dangling bonds and the bonding reconstruction at the NW surface. The surface reconstruction also has an impact on the atoms in the wire core—this also adds to the wire free energy. The thicker the whisker the smaller should be $\varepsilon_{\text{free}}$, as the ratio of the number of atoms at the surface to the total number of atoms in the wire decreases with the radius. In figure 3 the results of the calculated free energies for GaAs NWs with different diameters and structures are collected. In agreement with expectations, $\varepsilon_{\text{free}}$ decreases with the diameters of the NWs for all structures. One observes, however, that for a given NW diameter, the lowest free energy corresponds always to the wz(0001) NW. None of the directions for zb NWs with diameters up to about 20 Å is preferred. For thicker zb NWs, the lowest free energy has been obtained for the ones with the axis along the (111) direction [16]. In figure 4 similar results for InAs wz(0001) and zb(111) NWs are presented. The obtained results are in agreement with the fact that most of the experiments report the growth of the III–V semiconductor NWs in wz(0001) or zb(111) structures.

To calculate the free energy for thicker wz(0001) and zb(111) NWs (with diameters larger than 5 nm), we assume that the total energy of such wires can be well approximated by the sum of bulk and bulk surface values. This assumption is based on the following observation: we note that at the {12.0}, surfaces of wz(0001) NWs the atoms are positioned in a threefold coordination, similar to the surface of bulk material in this direction. For zb(111) NWs, the same applies to all atoms at the {110} surface except for the few twofold-coordinated As atoms situated at the edges of the hexagonal NW cross section. The number of the latter is, however, constant and does not depend on the diameter of the wire and their contribution to the total energy decreases with diameter. Thus, the thicker the zb(111) NWs, the more justified is our assumption.

We first consider the zb and wz bulk structures for both GaAs and InAs materials. The minimization of the calculated total energy of the bulk unit cell leads to the following lattice constants of the bulk zb structures: $a^{\text{GaAs}} = 5.721$ Å and $a^{\text{InAs}} = 6.166$ Å. For the wz structures we obtain: $a^{\text{GaAs}} =$

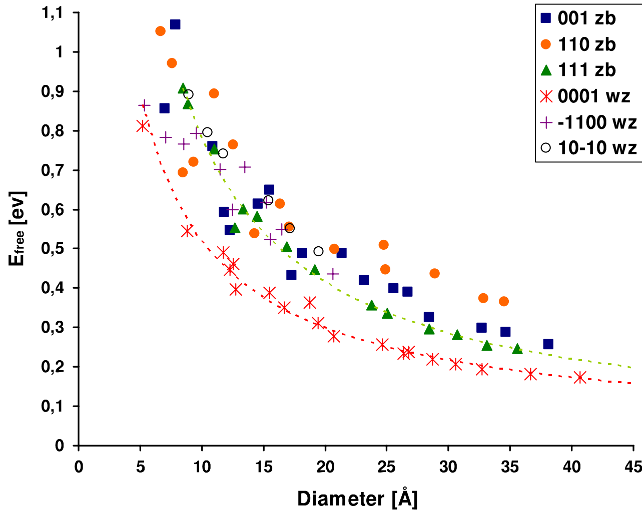

Figure 3. Dependence of the wire free energy on the GaAs NW diameter for all studied structures. To draw attention to the lowest energy structures (wz(0001) and zb(111)), the appropriate points are connected with dotted, green (zb) or red (wz), lines.

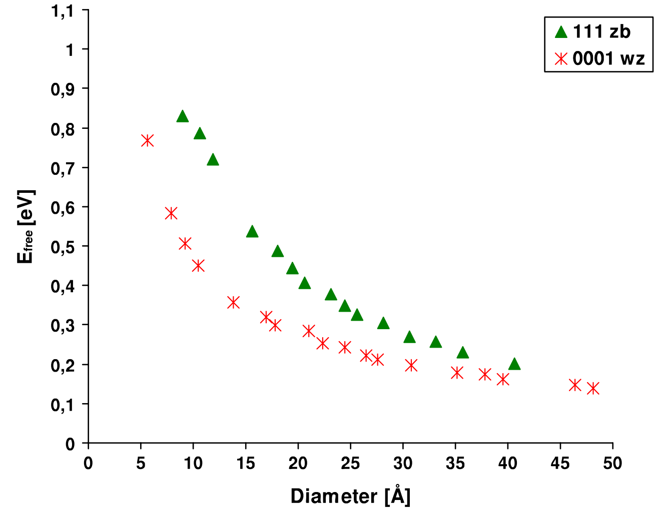

Figure 4. Dependence of the wire free energy on the InAs NW diameter.

4.029 Å, $c^{\mathrm{GaAs}} = 6.652$ Å and $a^{\mathrm{InAs}} = 4.353$ Å, $c^{\mathrm{InAs}} = 7.140$ Å. For the bulk surface energy calculations, we consider a relaxed slab of either zb or wz structure, in {110} and {12.0} orientation, respectively, with the unit cell lateral dimensions determined by the above lattice constants. Our slabs consist of nine atomic layers, each composed of both Ga(In) cations and As anions, and a vacuum region with the thickness equivalent to about seven monolayers. The atoms at the central, fifth, layer of the slab are fixed at their ideal bulk positions. The Brillouin zone is sampled with 48 special k points. The energy $\gamma_{\mathrm{surface}}$ of the surface with area A^{S} is defined as [17]

$$\gamma_{\mathrm{surface}} A^{\mathrm{S}} = E_{\mathrm{slab}} - \mu^{i}_{\mathrm{bulk}} N_{\mathrm{pair}}, \qquad (2)$$

where E_{slab} is the total energy of the slab and μ^{i}_{bulk} is the energy per anion–cation pair of the ith bulk material (i denotes wz or zb). Here N_{pair} is the number of atomic pairs in the slab. Using (2) we obtain: for GaAs, the surface energy in zb is equal to 37 meV Å^{-2} and 33 meV Å^{-2} for the wz structure. For InAs, the surface energy is equal to 29 meV Å^{-2} and 25 meV Å^{-2} in zb and wz structures, respectively. These values, which have been obtained within the general gradient approximation (GGA), are considerably lower than those obtained by previous local-density approximation (LDA) calculations of the surface energy in GaAs [17, 18] and InAs [19]. In the cited papers the energy of the relaxed {110} surface in GaAs exceeded 50 meV Å^{-2} and was equal to 41 meV Å^{-2} in the case of InAs. These differences originate, however, solely from using other exchange correlation energy approximations and disappear when in the calculation of $\gamma_{\mathrm{surface}}$ we apply LDA to the exchange correlation functional or projected augmented waves (PAW) method. Despite this well-known uncertainty of energy values obtained by the *ab initio* calculations, we believe that the results concerning free energy, i.e. the change in energies, are fully reliable.

Using equations (2) and (1) one observes that the wire free energy can now be approximated by the following equations:

$$\tilde{\varepsilon}_{\mathrm{free}} = \frac{\gamma_{\mathrm{surface}} A^{\mathrm{NW}}}{N_{\mathrm{pair}}}, \qquad (3)$$

for zb NWs, whereas for wz NWs one has to use

$$\tilde{\varepsilon}_{\mathrm{free}} = \frac{\gamma_{\mathrm{surface}} A^{\mathrm{NW}}}{N_{\mathrm{pair}}} + \mu^{w}_{\mathrm{bulk}} - \mu^{\mathrm{zb}}_{\mathrm{bulk}}. \qquad (4)$$

As shown in figure 5, for wz NWs the two methods of determining the free energy described above lead to very similar results and for wires thicker than 10 Å both values, $\tilde{\varepsilon}$ and ε, become practically equal. In contrast, for zb NWs (figure 6) the free energies $\tilde{\varepsilon}$ approximated by the bulk surface energy differ considerably from the calculated ε values up to diameters of about 50 Å. This is due to neglecting in the approximation the twofold-coordinated atoms with additional dangling bonds, which are present in the zb NWs, as was mentioned above. Still, one can see in figure 6 that the difference between the two curves, i.e. the contribution of the extra dangling bonds to the NWs free energy diminishes with the radius, and for diameters larger than 50 Å can indeed be neglected. Using this simple model, we predict that, for NWs with diameters smaller than 100 Å, the wurtzite structure should be still more energetically favourable. However, for NWs of such thickness the difference in free energies between wurtzite and zinc-blende becomes really small and NWs of both kinds of structures can appear, depending on the growth conditions. We have obtained the same behaviour for both GaAs and InAs wires. However, the energy differences between the zb and wz are bigger for GaAs, for all diameters. Thus, one can expect that the critical diameter for obtaining wz(0001) GaAs NW would be even higher than 100 Å. Finally, it should be noted that the above calculations are performed for a single one. Although several tests on longer unit cells did not reveal any differences with the obtained results for a single unit cell, a careful study of the dependence of the stability

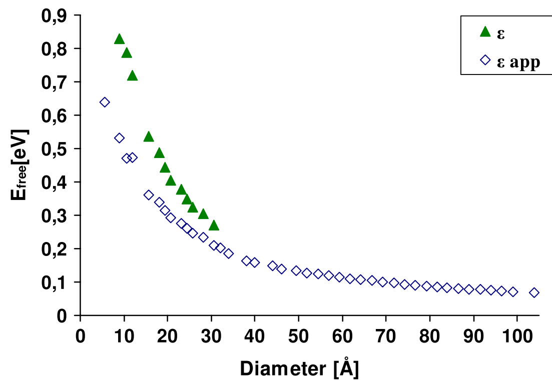

Figure 5. Dependence of the calculated and approximated wire free energy on the InAs NW diameter for wz structures.

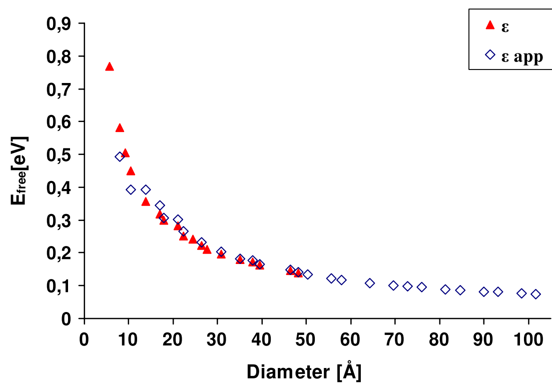

Figure 6. Dependence of the calculated and approximated wire free energy on the InAs NW diameter for zb structures.

and surface reconstruction on the unit cell dimension, for different configurations, should be made. Such calculations, unfortunately very costly, which, apart from removing possible constraints, allow considering other (like 4H) stackings are in progress.

3. Band structure

In this section we study the impact of the crystallographic structure (zb versus wz) on the NW band structure. Our calculations show that the main features of NW energy spectra for GaAs and InAs do not differ considerably. Although the bandgap and the details of the bands' shape depend on the wire diameters, these do not affect the differences between the zb and wz NWs band structure. Thus, for clarity we present and discuss the results for only one compound (InAs) and one nanowire radius (10 Å). The calculated energy spectrum for the zb(111) NW is presented in figure 7(a) and compared with the band structure calculated for the wz(0001) NW, shown in figure 8. First, we observe that in both cases the obtained energy bandgap in the NW is larger by about 1 eV than in the bulk. Although it is well known that the DFT accounts incorrectly for the excited electronic states of solids, and hence leads in general to far too small bandgaps, we believe again that this drawback does not affect the difference between the gaps in NW and bulk material (which has been demonstrated for InP NWs [20]). Moreover, one should indeed expect an increase of the bandgap in NWs, as a result of the confinement.

The {110} surface is the main cleavage surface of GaAs and has, therefore, been extensively studied (see [21] and the references therein). It is now well established that the relaxed {110} surface has (1×1) symmetry and fulfils the requirements of the electron-counting model, i.e. is semiconducting—since all As dangling bonds are filled, while the Ga dangling bonds are emptied at this surface, one does not expect additional states related to the {110} surface in the gap or conduction band. Despite this, for zb NWs we obtain additional states located in the bandgap with the Fermi level (red dashed–dotted line) pinned at these states. On the other hand, for the wz(0001) NWs such bandgap states are not found, as is expected when no extra electrons are introduced. In order to shed some more light on this problem, for the zb structure we calculate the density of charge generated by the additional states in the bandgap. The results of the calculation, presented in figure 7(b), clearly show

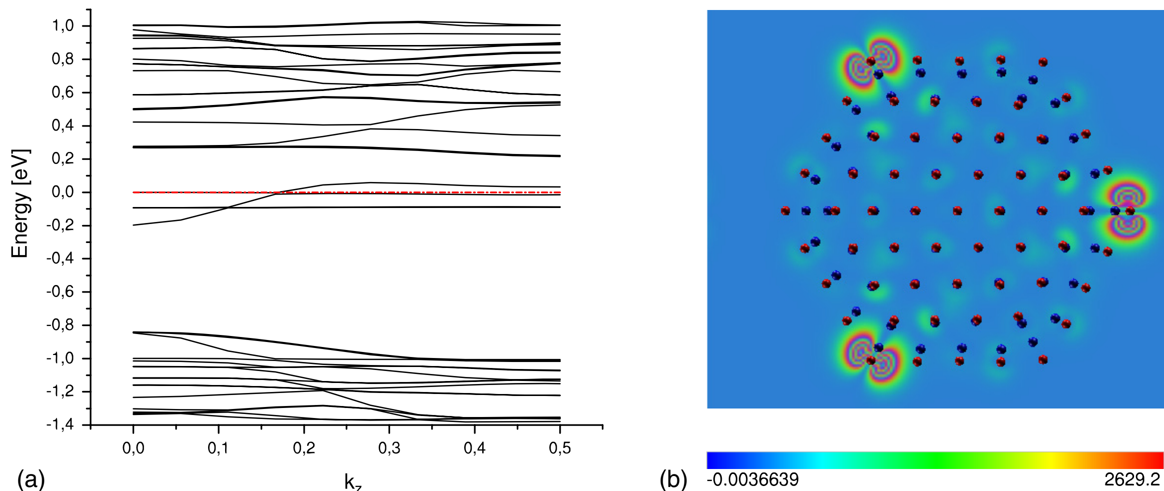

Figure 7. (a) Band structure of InAs nanowire in the zb structure with the diameter 20 Å. (b) The charge density for states in the gap, up to the Fermi level. The red (gray) balls denote the As anions whereas the blue (black) balls denote the In cations. The scale of colours corresponds to the value of the accumulated charge.

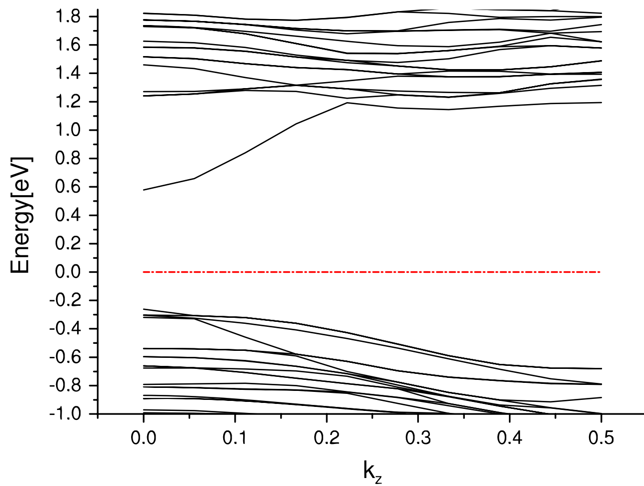

Figure 8. Band structure of InAs nanowire in the wurtzite structure with the diameter 20 Å.

an accumulation of the charge around the twofold-coordinated As atoms at the edges. This allows us to conclude that, in agreement with the situation in the bulk, there are no states in the gap related to the zb{110} or wz{12.0} surfaces: however, the extra dangling bonds at the edges of the zb wire cross section produce such states. It should be emphasized that this property of the twofold-coordinated atoms does not depend on the diameter of the wire, in contrast to their contribution to the wire total energy, described in the previous section. On the other hand, however, we expect that the extra states can be removed from the gap or added again by passivation with appropriate atoms, as shown in the case of InP in [22].

4. Conclusions

In summary, we have studied theoretically the stability of various GaAs and InAs NWs. Our calculations indicate that the energy paid for the surface reconstruction in the wire takes the lowest value for NWs grown along (0001) in the wz structure. Therefore, this seems to be the preferred configuration for the growth of thin, with diameters up to 50 Å, GaAs and InAs wires. For larger diameters we also obtain low free energy for the zb NWs, grown along the (111) direction. For NWs with diameters of about 100 Å, the free energies of wz(0001) and zb(111) structures become nearly equal. Similar behaviour was also obtained in the case of InP [12]. The calculations of the band structure of the NWs show a 1 eV increase of the energy gap, as compared to the bulk materials. In the zb structures, additional states localized in the bandgap are predicted. The calculated charge density for these states up to the Fermi level shows an accumulation of charge around the twofold-coordinated As atoms. This indicates that the extra dangling bonds of these atoms are responsible for the surface states in the gap.

Acknowledgments

We thank Hadas Shtrikman, Moty Heiblum, Ronit Popovitz-Biro and Andrey Kretinin for valuable discussions and experimental support. This work was partly supported by EU-Transnational Access programme, EU project RITA-CT-2003-506095. All computations were carried out exploiting the resources and software of the Informatic Centre Tricity Academic Computer Net (CI TASK) in Gdansk.

References

[1] Bryllert T, Wernersson L-E, Fröberg L and Samuelson L 2006 *IEEE Electron Device Lett.* **27** 323–5
[2] Bryllert T, Wernersson L-E, Fröberg L and Samuelson L 2006 *Nanotechnology* **17** S227–30
[3] Duan X F, Huang Y, Cui Y, Wang J and Lieber C M 2001 *Nature* **409** 66–71
[4] Cui Y and Lieber C M 2001 *Science* **291** 851–3
[5] Huang Y, Duan X F, Cui Y, Lauhon L J, Kim K-H and Lieber C M 2001 *Science* **291** 630–33
[6] Björk M T, Ohlsson B J, Thelander C, Persson A, Deppert K, Wallenberg L R and Samuelson L 2002 *Appl. Phys. Lett.* **81** 4458–60
[7] Thelander C, Mårtensson T, Ohlsson B J, Larsson M W, Wallenberg L R and Samuelson L 2003 *Appl. Phys. Lett.* **83** 2052–4
[8] Dubrowskii V G and Sibirev N V 2008 *Phys. Rev.* B **77** 035414
[9] Glas F, Harmand J-C and Patriarche G 2007 *Phys. Rev. Lett.* **99** 146101
[10] Akayama T, Sano K, Nakamura K and Ito T 2006 *Japan. J. Appl. Phys.* **45** L275–8
[11] Leitsmann R and Bechistedt F 2007 *J. Appl. Phys.* **102** 063528
[12] Akayama T, Nakamura K and Ito T 2006 *Phys. Rev.* B **73** 235308
[13] Kresse G and Hafner J 1993 *Phys. Rev.* B **47** R558
[14] Kresse G and Hafner J 1996 *Phys. Rev.* B **54** 11169
[15] Perdew J P, Burke K and Wang Y 1996 *Phys. Rev.* B **54** 16533–9
[16] Bukała M, Galicka M, Buczko R and Kacman P 2007 *Acta Phys. Pol.* A **112** 425–30
[17] Moll N, Kley A, Pehlke E and Scheffler M 1996 *Phys. Rev.* B **54** 8844–55
[18] Qian G-X, Martin R M and Chadi D J 1988 *Phys. Rev.* B **37** 1303–7
[19] Pehlke E, Moll N, Kley A and Scheffler M 1997 *Appl. Phys.* A **65** 525–34
[20] Schmidt T M, Miwa R H, Venezuela P and Fazzio A 2005 *Phys. Rev.* B **72** 193404
[21] Haugk M, Elsner J and Frauenheim Th 1997 *J. Phys.: Condens. Matter* **9** 7305–15
[22] Schmidt T M 2006 *Appl. Phys. Lett.* **89** 123117